Proceedings of the 21st ICSMGE, Vienna, Austria, 14 – 19 June 2026. Pistrol, Adam & Schweiger (eds.)
Published by: ÖGG, Austrian Society for Geomechanics, Salzburg, Austria, ISBN 978-3-9503898-4-5
https://doi.org/10.53243/ICSMGE2026-2286

Site Amplification Characteristics Across Budapest: A Comparative Analysis with Eurocode Spectra

Al-Azazmeh Ahmad[1*]
Budapest University of Technology and Economics, Azazmeh9999@edu.bme.hu

András Mahler[1*]
Budapest University of Technology and Economics, mahler.andras@emk.bme.hu

[1*]*Dept. of Geotechnical Engineering, Budapest University of Technology and Economics, Budapest, Hungary*

ABSTRACT: This study investigates site amplification effects across Budapest, developing typical amplification functions and design spectra for the city. Site-specific response analyses were conducted on diverse soil profiles to assess local seismic amplification. The research is supported by an extensive dataset, including 80 CPTu soundings and 35 in situ seismic measurements from 11 sites. Seismic data were primarily obtained through Multichannel Analysis of Surface Waves (MASW), complemented by Seismic Cone Penetration Tests (SCPT) and surface tomography. A comprehensive database of 1304 paired CPT readings and shear wave velocity measurements supports the analysis, enabling detailed subsurface characterization. The derived amplification functions and design spectra were compared with Eurocode 8 (EC8) guidelines, revealing deviations and opportunities to refine current seismic design practices. The findings highlight the relationship between subsurface properties and seismic response, offering critical insights for urban seismic hazard assessment and engineering design in Budapest. This study advances the understanding of site-specific seismic behavior, supporting infrastructure resilience and safety. The results have practical implications for updating regional seismic codes and improving earthquake-resistant design strategies in urban environments.

KEYWORDS: Site amplification; seismic response; design spectrum; Eurocode 8; Budapest; shear wave velocity.

1 INTRODUCTION

Seismic ground motions are strongly influenced by local site conditions, particularly in urban areas where soft soils can amplify shaking. These site effects depend on subsurface layering, shear wave velocity (V_s), and soil nonlinearity under cyclic loading (Julie Régnier, 2018) (Hashash, 2010). Standard classification schemes, such as Eurocode 8 (EC8), often use V_{s30} to estimate site amplification, but this simplification may overlook important characteristics of site response (Szilvágyi, et al., 2017) (Al-Azazmeh & Mahler, 2025a).

Budapest lies within the Pannonian Basin, a seismically moderate region with estimated peak ground accelerations (PGA) between 0.08 g and 0.15 g for a 475-year return period (Szilvágyi, et al., 2017). The city's subsurface consists of variable Quaternary and Tertiary deposits, making seismic response spatially heterogeneous. While previous studies have examined site effects at individual locations, a city-wide assessment using high-resolution geotechnical and geophysical data is lacking (Al-Azazmeh & Mahler, 2024).

This study presents an evaluation of site amplification for the central and eastern parts of Budapest, and because most seismic test locations are situated on the Pest side, the results primarily represent the response of the deposits of this region, using a dataset of 80 CPTu soundings and 35 seismic tests (MASW, SCPT, and surface tomography) from 11 locations (Figure 1). Over 1300 paired V_s –CPT points form the basis for detailed 1D nonlinear response analyses. Input bedrock motions consistent with EC8 design spectra were applied to representative soil profiles to assess amplification trends and compare them with the recommendations of EC8 (Standardization, 2004) (Al-Azazmeh & Mahler, 2025b).

The aim is to identify where standard design spectra may underestimate or overestimate actual site response, and to provide geotechnical insights for improving seismic design across the city. Considering the number and spatial distribution of the sites, it can be stated that this study provides a good overview of the expected site amplifications.

Figure 1 Locations of CPTu and Seismic Test Sites Used for Site Amplification Analysis in Budapest.

2 SITE CHARACTERIZATION AND SEISMIC INPUT

2.1 *Geological Setting*

Budapest lies straddling two distinct geological regimes. The Buda side (west of the Danube) is dominated by hilly terrain underlain by karst-forming Triassic limestone and dolomite, featuring fault-induced thermal springs. In contrast, the Pest side comprises the flat-lying Pannonian Plain, covered with Quaternary alluvial sediments clays, silts, sands, and anthropogenic fill resulting from historical fluvial and aeolian deposition. These stratigraphic contrasts, often occurring over short lateral spans, are critical for seismic ground response studies.

2.2 *Geotechnical and Geophysical Investigations*

To capture this subsurface variability, we carried out measurements at 11 sites across Budapest, using:

- CPTu (Cone Penetration Test with pore pressure measurement) –80 soundings distributed throughout both sides of the city.
- MASW (Multichannel Analysis of Surface Waves) –25 measurements.
- SCPT (Seismic CPT) – 10 tests combining geotechnical and V_s profiling.

These methods were chosen based on established practice in the region. MASW surveys used 48-channel geophone arrays with 3 m spacing; data processing followed f–k domain inversion to yield 1D V_s profiles. SCPT tests employed downhole geophone sensors to resolve near-surface shear wave velocities with high vertical resolution.

2.3 *V_s Profiles: Processing and Interpretation*

Typical V_s -depth profiles revealed the following trends:

- 0–4 m: $V_s \approx$ 140–240 m/s, soft, possibly fine-grained soils typically Holocene age or fill materials
- 4–14 m: $V_s \approx$ 160–330 m/s, dominantly Pleistocene Danube deposits in the forms of silts, silty sands or sands.
- 14–32 m: $V_s \approx$ 300-600 m/s, Dense Tertiary layers, compacted sands, dense silty layers, or weathered bedrock-like material, frequently indicating a strong impedance contrast a key parameter driving site amplification.

Integration of CPTu-derived soil behavior indices with MASW profiles allowed for refined stratification and validation of layering features.

2.4 *Site Classification and EC8 Parameters*

Using V_{s30} estimates from the compiled dataset and referencing the Hungarian National Annex to Eurocode 8, most sites fell into Soil Class C (V_{s30} = 180–360 m/s), with some localized B or D classes. EC8's design PGA for Budapest is 0.12 g, which we adopted in defining a target response spectrum, including corner periods TB = 0.25 s, TC = 0.75 s, and TD = 3.75 s (SSA format).

2.5 *Ground Motion Selection and Target Spectrum*

Seven seismic records were selected from the SHARE database Table 1, targeting events in the M_w 5.2–6.0 range and encompassing various faulting styles and source-to-site distances. These records feature spectral acceleration of 0.15–0.25 g in the 0.2–0.6 s range and align well with the EC8-based target spectrum.

Table 1 Selected Seismic Records (SHARE Database)

Event ID / Name	***Station***	***Magnitude (Mw)***	***Mechanism***	***Vs30 (m/s)***
Hollister-04 (1986)	SAGO	5.45	Strike slip	609
IT-2009-0102	BZZ	5.50	Normal	679
IT-1997-0137	CSC	5.60	Normal	698
IT-2009-0121	AQG	5.40	Normal	696
EMSC-20161026	CSC	6.00	Normal	698
GR-1993-0006	KYPA	5.20	Reverse	822
IT-2009-0121	AQP	5.40	Normal	836

3 SITE RESPONSE ANALYSIS

3.1 *Methodological Framework*

To evaluate site-specific seismic amplification at the sites, a series of nonlinear one-dimensional (1D) site response analyses were conducted. The methodology was selected to capture the strain-dependent behavior of soils under seismic loading, which is often underestimated in linear or equivalent-linear models, especially at moderate-to-high shaking levels (Hashash, 2010); (Julie Régnier, 2018). The modeling framework adheres to the principles of performance-based earthquake engineering (PBEE), in which local soil conditions, ground motion variability, and strain-compatible soil properties are jointly considered.

Nonlinear analyses were implemented using the software DEEPSOIL, which support hyperbolic-modulus reduction and hysteretic damping formulations. Each soil profile was discretized into 0.5–1.0 m thick layers, with dynamic soil properties assigned based on seismic in situ measurements and CPTu based empirical correlations. Modulus reduction and damping curves were defined based on earlier experiences. (Vucetic & Dobry, 1991) (Darendeli, 2001).

3.2 *Soil Profile Development and Stratigraphy*

Soil profiles extending to 60 meters were developed at each site using borehole logs, CPTu data, and shear wave velocity profiles, with in-situ measurements covering the upper 25–30 meters and deeper layers extrapolated from regional experience. A sensitivity assessment indicated that site amplification in the critical short-to-medium period range is predominantly controlled by the measured upper layers, meaning that the response envelope generated by the seven diverse input motions sufficiently captures the uncertainty associated with the extrapolated deep strata. The models, typically comprising 20–25 layers, were assigned specific dynamic properties including shear wave velocity, unit weight, undrained shear strength, plasticity index, and groundwater depth derived directly from geophysical tests and local correlations. This stratigraphy reflects the transition from soft surface sediments to denser deep deposits, resting on an assumed bedrock with a shear wave velocity of 800 m/s.

3.3 *Constitutive Modeling and Material Behavior*

Each soil layer was assigned strain-compatible nonlinear dynamic properties, governed by:

- Modulus reduction (G/G_{max}) curves, and
- Material damping (ξ) curves,

following the widely used relationships of (Darendeli, 2001). These are pressure-dependent and consider confining stress, PI, OCR, and strain level, making them appropriate for both cohesive and cohesionless soils. The curves were implemented using the modified hyperbolic backbone model, with Masing-type hysteresis to represent cyclic loading-unloading behavior.

This constitutive framework captures:

- Stiffness degradation at increasing strain amplitudes.
- Energy dissipation due to hysteretic damping.

- Layer-specific transitions in stiffness, relevant for wave amplification and trapping.

3.4 *Numerical Configuration and Boundary Conditions*

The site response simulations applied seven spectrally matched ground motion records from the SHARE database, with PGA = 0.12g. Input motions were applied as outcrop motions at the base of each soil column. The following modeling settings were used:

- Time step (Δt): 0.005 seconds.
- Baseline correction: linear trend and mean removal.
- Filtering: 0.1–20 Hz bandpass applied.
- Boundary conditions: elastic half-space or compliant base model, depending on underlying formation characteristics.

The base impedance condition was chosen based on the estimated V_s of the lowest layer, following best practices from both NGA-East and PRENOLIN benchmark studies (Julie Régnier, 2018); (Stewart, et al., 2014).

3.5 *Model Output Parameters*

Key outputs extracted from each simulation include:

- Surface and base acceleration time histories.
- 5%-damped acceleration response spectra (Sa).
- Amplification functions (S_a_surface / S_a_base) as a function of frequency.
- Maximum shear strain profiles, to evaluate nonlinear effects.
- Transfer functions and site period (T_0).

Results were aggregated across all sites and compared against Eurocode 8 spectra to evaluate conservatism, frequency-dependent deviations, and amplification trends tied to local soil conditions.

3.6 *Site response analysis results*

Figure 2 illustrates the spectral amplification ratios (surface/bedrock) at Site 2, computed from nonlinear 1D site response analyses using seven spectrum-matched ground motions. The soil column at this location extends to a depth of 60 m, where seismic bedrock was defined based on a shear wave velocity threshold of 800 m/s. Each colored line in the plot corresponds to a single ground motion, while the red dashed curves indicate ±1 standard deviation bounds.

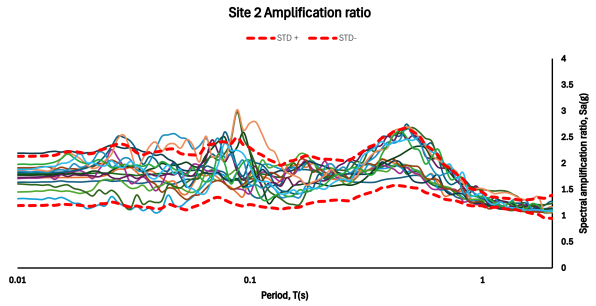

Figure 2 Spectral Amplification at Site 2: Multi-Record Average.

The analysis reveals a distinct amplification peak occurring between 0.28 and 0.36 seconds, with maximum spectral ratios exceeding 2.8 in some cases. This period range closely corresponds to the fundamental natural period of the soil profile, estimated using the simplified relation T=4H/ V_s . the computed resonance period lies between 0.34 and 0.38 s closely aligned with the observed amplification maxima. This confirms that vertical impedance contrast and layered stiffness transitions are the dominant contributors to resonance-induced amplification at Site 2.

Secondary amplification is also observed at very short periods (T < 0.1 s), with ratios up to 2.2. This period coincides well with the fundamental natural period of the near-surface low-stiffness layers. These high-frequency amplifications may be critical for low-rise structures.

Beyond 1.0 s, spectral amplification ratios trend toward unity or fall below it, indicating minimal long-period energy build-up. This behavior suggests that the site's ability to amplify longer-period components is limited by the moderate stiffness gradient and lack of deep soft sediments.

3.7 *Average and Envelope Amplification Patterns*

As shown in Figure 3 (All Sites Amplification Ratio), the computed surface-to-bedrock amplification functions exhibit considerable variability in the short-period range (T < 0.8 s), while gradually converging toward unity for longer periods. The solid black line represents the average spectral amplification ratio across all sites, while the red dashed curves indicate ±1 average standard deviation bounds.

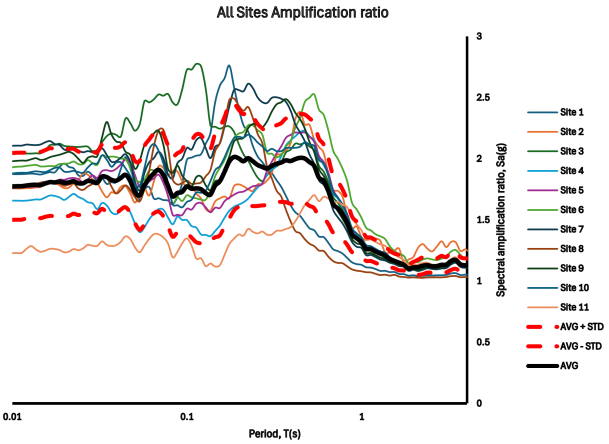

Figure 3 Surface Spectral Acceleration Across Sites Compared to Average Input Motion

A dominant peak is observed between 0.25 and 0.35 seconds, where the mean amplification ratio approaches 2.2, localized amplification peaks were observed at specific sites, with spectral ratios exceeding 2.6. The spread in individual site responses in the T<0,6 range, most notably Site 2 and Site 6, highlights the sensitivity of site response to the variability, impedance contrasts in the upper 20-30 meters.

Beyond 1.2 seconds, the average amplification ratio declines and stabilizes near 1.1, indicating minimal amplification at longer periods. The low variability in this range suggests a uniform attenuation effect across deeper or stiffer subsoils, and lower energy transfer from input motions in the long-period band.

3.8 *Surface Amplification Relative to Input Motions*

Figure 4 depicts surface response spectra relative to the average ground motion. Peak surface amplifications occur between 0.2 and 0.4 seconds, reaching 0.5g approximately double the input motion which poses a potential risk to low- and mid-rise structures in this spectral window[2]. While the average curve follows the expected decay pattern, substantial inter-site variation persists; notably, Sites 3 and 6 consistently exhibit the highest responses, a behavior attributed to their low V_{s30} values and thick near-surface cohesive layers.

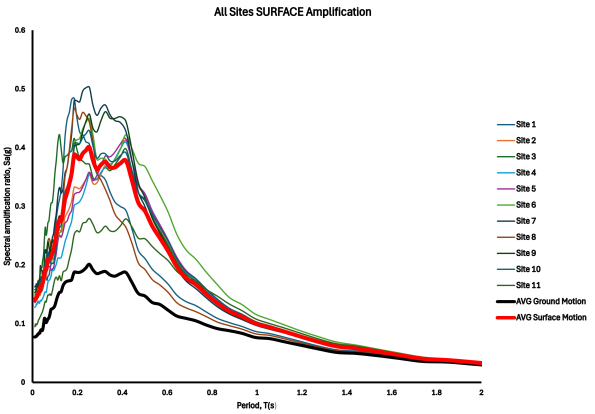

Figure 4 Spectral Amplification Ratios Across All Sites: Mean, Variability, and Site-Specific Trends

3.9 *Implications for Seismic Design Practice*

The Comparative analysis reveals that seismic amplification in Budapest is not uniform, even among sites with similar V_{s30} values, indicating that standard EC8 classification inadequately captures local stratigraphic effects. Deviations are most critical in the 0.2–0.5s range, where median amplification reaches approximately 2.0, exceeding EC8 Type 1 limits by 25–80% and signaling a significant underestimation of resonance-driven response in the National Annex. While the observed behavior aligns more closely with Type 2 spectra, it remains distinct; short-period peaks approach upper Type 2 values, whereas long-period amplification ($T \geq 1.0$ s) drops to 1.1–1.3, falling well below the standard 1.7–2.7 range[3]. These findings highlight the necessity of adopting site-specific design spectra for critical infrastructure to address the substantial inter-site variability and specific resonance characteristics of the city's alluvial deposits.

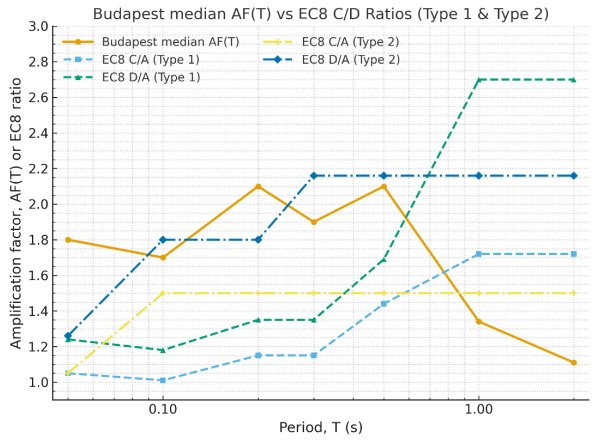

Figure 5 Comparison of Budapest median amplification factors AF(T) with EC8 C and D ratios for Type 1 and Type 2 spectra.

4 CONCLUSIONS

This study provides a detailed assessment of seismic site amplification for the central and eastern parts of Budapest (Pest side), combining in-situ geotechnical data with nonlinear 1D site response analyses. Using 11 representative profiles and multiple spectrum-matched input motions, consistent amplification peaks were identified between 0.25 and 0.4 seconds, closely linked to the fundamental periods of soft soil layers common in the region.

The results reveal significant deviations from Eurocode 8 spectra, particularly for sites nominally classified as Soil Class C or D. While the observed behavior aligns more closely with Type 2 spectra, the standard Type 1 spectra prescribed in the Hungarian National Annex were found to underestimate resonance-driven amplification by up to 80% in the short-period range. This highlights the limitations of V_{s30}-based classifications and underscores the importance of accounting for detailed stratigraphy and impedance contrasts in seismic design.

Inter-site variability was most pronounced in the short-period range, aligning with the resonance periods of typical residential and mid-rise buildings. These findings support the need for site-specific design spectra and refined microzonation to ensure safer, more resilient urban development. By integrating high-resolution subsurface data with rigorous dynamic modeling, this research offers practical tools and insights for improving seismic hazard assessment and infrastructure design in Budapest and similar urban regions.

5 REFERENCES

Al-Azazmeh, A. & Mahler, A., 2024. Development of CPT-Vs correlations for soft quaternary clays of Szeged city Hungary. In: *Geotechnical Engineering Challenges to Meet Current and Emerging Needs of Society.* Lisbon, Portugal: s.n.

Al-Azazmeh, A. & Mahler, A., 2025a. Nonlinear Site Response Analysis in District XIII, Budapest. *Slovak Journal of Civil Engineering,* 33(3), pp. 54-61.

Al-Azazmeh, A. & Mahler, A., 2025b. Modified Correlations to Predict Shear-wave Velocity Using Cone Penetration Test Data for Hungary. *Periodica Polytechnica Civil Engineering,* 69(4), pp. 1311-1320.

Darendeli, M. B., 2001. *Development of a new family of normalized modulus reduction and material damping curves,* Austin, TX: s.n.

Hashash, Y. M. A. P. C. &. G. D. R., 2010. *Recent Advances in Non-Linear Site Response Analysis..* s.l., s.n.

Julie Régnier, L. B. P. B. E. B. F. H. H. K. D. S. P. A. A. A. D. A. D. B. L. C. A. C. F. D. A. E. G., 2018. International Benchmark on 1D Nonlinear Site-Response Analysis—Validation Phase Exercise. *Bulletin of the Seismological Society of America,* 108(2), pp. 876-900.

Standardization, E. C. f., 2004. *Eurocode 8: Design of structures for earthquake resistance – Part 1: General rules, seismic actions and rules for buildings,* Brussels: CEN.

Stewart, J. P., Afshari, K. & Hashash, Y. M. A., 2014. *Guidelines for performing hazard-consistent one-dimensional ground response analysis for ground motion prediction,* Berkeley: s.n.

Szilvágyi, Z. et al., 2017. Ground Response Analyses in Budapest Based on SiteInvestigations and Laboratory Measurements. *World Acad. Sci. Eng. Technol. Int. J. Environ. Chem. Ecol. Geol. Geophys. Eng.,* Issue 11, pp. 307-317.

Vucetic, M. & Dobry, R., 1991. Effect of soil plasticity on cyclic response. *Journal of Geotechnical Engineering,* 117(1), p. 89–107.